

**Proteasome inhibitors potentiate etoposide-induced cell death in human astrocytoma
cells bearing a mutated p53 isoform**

Stefania Ceruti, Alessia Mazzola, Maria P. Abbracchio

Laboratory of Molecular and Cellular Pharmacology of Purinergic Transmission -
Department of Pharmacological Sciences - School of Pharmacy - University of Milan -
Via Balzaretti, 9 - 20133 Milan, Italy (SC, AM, MPA)

Running title: Proteasome inhibition and apoptosis

Corresponding author:

Prof. Mariapia Abbracchio

Department of Pharmacological Sciences

University of Milan

Via Balzaretti, 9

20133 MILAN, ITALY

Tel. +39-02-50318310

Fax. +39-02-50318284

email mariapia.abbracchio@unimi.it

36 TEXT PAGES

2 TABLES

8 FIGURES

37 REFERENCES

198 WORDS IN ABSTRACT

691 WORDS IN INTRODUCTION

1504 WORDS IN DISCUSSION

Abbreviations: Ac-DEVD-fmk, N-Acetyl-Asp-Glu-Val-Asp-fluoromethylketone; Ac-DEVD-pNA, N-Acetyl-Asp-Glu-Val-Asp-paranitroaniline; Ac-IETD-fmk, N-Acetyl-Ile-Glu-Thr-Asp-fluoromethylketone; Ac-IETD-pNA, N-Acetyl-Ile-Glu-Thr-Asp-paranitroaniline; Ac-LEHD-fmk, N-Acetyl-Leu-Glu-His-Asp-fluoromethylketone; Ac-LEHD-pNA, N-Acetyl-Leu-Glu-His-Asp-paranitroaniline; Ac-VDVAD-fmk, N-Acetyl-Val-Asp-Val-Ala-Asp-

fluoromethylketone; Ac-VDVAD-pNA, N-Acetyl-Val-Asp-Val-Ala-Asp-paranitroaniline;
AllM, N-acetyl-Leu-Leu-Met-al; AllN, N-Acetyl-Leu-Leu-NorLeu-al; Ca-074Me, L-3-*trans*-
(Propylcarbamyl)oxirane-2-carbonyl)-L-isoleucyl-L-proline methyl ester; Eto, Etoposide;
E64, *trans*-Epoxy succinyl-L-leucylamido(4-guanidino)butane; JC-1, 5,5',6,6'-tetrachloro-
1,1',3,3'-tetraethylbenzimidazolcarbocyanine iodide; LLnV, N-Acetyl-Leu-Leu-NorVal-al;
PFT- α , pifithrin- α .; zVAD-fmk, N-Benzoyloxy carbonyl-Val-Ala-Asp-fluoromethylketone

Section: Cellular and Molecular

ABSTRACT

Resistance to anti-cancer agents is often due to defects of intracellular pathways of cell death. Thus, the identification of the apoptotic pathways that can still be recruited by chemotherapeutic agents in cancerous cells can disclose new opportunities to treat malignancies. Here we show that human astrocytoma ADF cells (which are resistant to “mitochondriotropic” agents as well as to the anti-neoplastic drug Etoposide and to proteasome inhibitors when utilized alone) undergo dramatic apoptotic death when exposed to a combination protocol based on the use of Etoposide in the presence of proteasome inhibitors. Sensitization to cell death involved an auto-amplifying loop of caspase activation, where the “executioner” phase of apoptosis was sustained by a cooperation of caspases -2, -9, -8 and -3. We also show that sensitization of cells to the combination protocol involved the nuclear relocalization of p53, despite the presence of a polymorphism in its DNA-binding domain, suggesting the likely induction of p53-dependent pro-apoptotic genes. Conversely, p53 phosphorylation on Ser-15 did not play any role in apoptosis. In conclusion, use of Etoposide in combination with proteasome inhibitors may represent an effective strategy to restore sensitivity to apoptosis in human astrocytoma cells bearing multiple defects of intracellular apoptotic pathways.

INTRODUCTION

The discovery of the central role played by the proteasome complex in controlling cell survival and cell death has led to the intuition that the pharmacological manipulation of its activity might represent a new and powerful approach to cancer therapy (Almond and Cohen, 2002). The proteasome controls the expression of transcription factors, such as NF- κ B, p53, c-Jun, and c-Fos that are critically involved in cell proliferation and differentiation. Moreover, the ubiquitin-proteasome system regulates cellular sensitivity to cell death by controlling the levels of proteins directly involved in the apoptotic process, such as members of the Bcl₂ family, inhibitor of apoptosis proteins (IAPs) and caspases (Almond and Cohen, 2002).

Proteasome inhibitors have been synthesized which have been extensively used both in pre-clinical and clinical studies. Small aldehydic peptides (i.e., N-acetyl-Leu-Leu-Met-al, N-Acetyl-Leu-Leu-NorLeu-al, and N-Acetyl-Leu-Leu-NorVal-al, known as ALLM, ALLN, and LLnV, respectively) have been exploited as useful pharmacological tools in in vitro models to characterize the role of the proteasome complex in cancer cells (Henderson et al., 2005). Indeed, a selective boronic acid proteasome inhibitor (bortezomib; Adams and Kauffman, 2004) has currently entered the clinical use for the treatment of relapsed or refractory multiple myeloma. Proteasome inhibitors exert their effects either per se, or can sensitize cancer cells to the effects of other cytotoxic agents (e.g., gemcitabine and TRAIL; Leverkus et al., 2003; Denlinger et al., 2004; Nencioni et al., 2005) by recruiting intracellular pathways of apoptosis (for review, see Mendoza et al., 2005). However, in cancer cells, some of these pathways are often defective, due to single or multiple mutations in key proteins controlling cell survival and death (e.g., p53 or caspases; Jäättelä, 2004). Thus it becomes extremely important to verify whether any chosen anti-cancer agent still retains the ability of inducing cell death in cellular models carrying mutations of apoptotic pathways.

In this respect, human astrocytoma ADF cells can be taken as an useful in vitro model to explore the pro-survival strategies implemented by a highly aggressive type of cancer, and to disclose the cell death pathways that are still functional in these cells, and can thus be recruited by anti-cancer drugs. In this respect, we have previously validated this cellular model as an adequate experimental system to study the alterations of apoptotic mechanisms in cancer cells by demonstrating that ADF cells are resistant to agents acting through the “classical” mitochondrial cell death pathway (e.g., Betulinic Acid, BetA), due to the presence of a mutated form of caspase-9 (Ceruti et al., 2005). Nevertheless, the ability of ADF cells to undergo programmed cell death could be restored by exposure to the anti-leukemic agent 2-chloro-2'-deoxyadenosine, which was able to activate a caspase-2-dependent pathway of apoptosis (Ceruti et al., 2003). At present no data are available for this astrocytoma cell line regarding the functionality of other proteins crucially involved in cell survival and cancer development (e.g., p53).

On this basis, in this paper, we have evaluated the possible effects of small aldehyde proteasome inhibitors on ADF cell survival when utilized either alone or in combination with the anti-cancer agent Etoposide (Eto, VP-16). This topoisomerase II inhibitor is widely used as anti-cancer agent in various human tumors, and was chosen based on clinical data showing its possible use as second line chemotherapy in patients with recurrent malignant glioma (Watanabe et al., 2002; Korones et al., 2003). Here we show that ADF cells are resistant to both proteasome inhibitors and Eto when utilized alone, but are highly sensitive to a combination of Eto+proteasome inhibitors, which activate the caspase-2-dependent pathway of death. Moreover, we have sequenced the p53 protein isoform expressed by ADF cells, and characterized its role in apoptosis in our experimental model. We also show that, despite the presence of a mutation in the DNA binding domain, the nuclear re-localization of the p53 protein is involved in induction of cell death. Thus, we suggest that exposure to proteasome

inhibitors may represent a highly effective protocol of sensitization to anti-cancer agents also in cancer cells bearing mutations of several cell death pathways. Although caution should be taken in translating *in vitro* data to *in vivo* situations, our observations may disclose new opportunities to overcome resistance to chemotherapy.

METHODS

Chemicals

Etoposide (Eto), N-acetyl-Leu-Leu-Met-al (AllM), N-Acetyl-Leu-Leu-NorLeu-al (AllN), N-Acetyl-Leu-Leu-NorVal-al (LLnV; MG115), E64 (*trans*-Epoxy succinyl-L-leucylamido(4-guanidino)butane), pepstatin, Ca-074Me (L-3-*trans*-(Propylcarbonyl)oxirane-2-carbonyl)-L-isoleucyl-L-proline methyl ester), calpastatin, pifithrin- α , epoxomicin, goat anti-mouse and goat anti-rabbit secondary HRP-conjugated antibodies were from Sigma-Aldrich (Milan, Italy). N-Acetyl-Asp-Glu-Val-Asp-paranitroaniline, N-Acetyl-Ile-Glu-Thr-Asp-paranitroaniline, N-Acetyl-Leu-Glu-His-Asp-paranitroaniline, and N-Acetyl-Val-Asp-Val-Ala-Asp-paranitroaniline (Ac-DEVD-pNA, Ac-IETD-pNA, Ac-LEHD-pNA, and Ac-VDVAD-pNA, respectively), the corresponding -fluoro-methyl-ketone-conjugated (-fmk) inhibitors, and N-Benzyloxy carbonyl-Val-Ala-Asp-fluoromethylketone (zVAD-fmk) were from Alexis Biochemicals (Vinci-Biochem, Vinci, Florence, Italy).

Cell culture and pharmacological treatments

Human astrocytoma ADF cells were maintained in culture in standard conditions (37°C, 95% humidity, 5% CO₂) in RPMI 1640 medium supplemented with 10% fetal bovine serum (FBS), 2 mM glutamine, 100 u/ml penicillin, 100 μ g/ml streptomycin and 1% non-essential aminoacids (all from Euroclone, Celbio, Italy), as previously described (Ceruti et al., 2000). Exposure to Eto was started 24 hours after plating cells on 6-well plates (600.000 cells/well). All the other pharmacological agents were added to cultures 30 minutes before Eto. In selected experiments, proteasome inhibitors were added at various time points (1-7 hours) after Eto, as indicated.

Cytofluorimetric Studies

Evaluation of apoptosis. The percentage of apoptotic cells in the total population (adhering + detached cells) was evaluated immediately at the end of the incubation period by means of propidium iodide (PI; Sigma Aldrich, Milan, Italy) staining of DNA followed by flow cytometric analysis, as previously described (Ceruti et al., 2003; 2005).

Analysis of Mitochondrial Membrane Potential. Changes in mitochondrial membrane potential ($\Delta\Psi_m$) induced in the total cell population by the various pharmacological treatments were analyzed by means of the fluorescent dye 5,5',6,6'-tetrachloro-1,1',3,3'-tetraethylbenzimidazolcarbocyanine iodide (JC-1, Molecular Probes, Società Italiana Chimici, Rome, Italy), as previously described (Ceruti et al., 1997; 2003). J-aggregate fluorescence was recorded by flow cytometry in the fluorescence channel 2 (FL2) and monomer fluorescence in the fluorescence channel 1 (FL1). Necrotic fragments were electronically gated out on the basis of morphological characteristics on the forward light scatter (FSC) versus the side light scatter (SSC) dot plot.

Detection of Caspase Activity

Caspase activity was measured by means of a spectrophotometric assay kit (CaspACE Assay System Colorimetric; Promega, Milan, Italy), following manufacturer's instructions with some minor modifications, as previously described (Ceruti et al., 2005). The evaluation of caspase activity was carried out in a 96-well plate in a total volume of 100 μ l, with a total amount of 70-150 μ g of protein in each sample and in the presence of tetrapeptide substrates conjugated to paranitroaniline (i.e., DEVD-pNA, LEHD-pNA IETD-pNA, and VDVAD-pNA in the case of caspase-3, -9, -8, and -2, respectively; final concentration 200 μ M). Extracts were incubated for 4 hours at 37°C, and released pNA was then measured in a

spectrophotometer at 405 nm. Each condition was run in triplicate, and for each experimental condition at least three independent experiments have been performed.

Subcellular fractionation and western blotting analysis

Whole-cell lysates (excluding nuclei) were prepared as previously described (Ceruti et al., 2005), while the separation of the cytosolic and nuclear subcellular fractions was performed as described in literature (Fortugno et al., 2002). Briefly, cells were collected by centrifugation (1,800 rpm for 10 minutes), washed with ice-cold PBS, lysed for 20 minutes at 4°C in Hepes Buffer (25 mM Hepes, pH 7.5, 100 mM KCl, 2 mM EGTA, 1% Triton X-100, in the presence of protease inhibitor cocktail), and further centrifuged at 900 g for 10 minutes at 4°C. The pellet was collected as nuclear fraction, whereas the supernatant was centrifuged at 2,000 g for 10 minutes at 4°C, and the resulting supernatant was collected as cytosolic fraction. For each experimental condition and subcellular fraction, 50-100 µg of proteins in each lane were size-fractionated by SDS-polyacrylamide gel electrophoresis in 12% acrylamide gel. After electroblotting onto nitrocellulose membrane, an overnight incubation with primary antibodies was performed. In particular, mouse anti-caspase-3 monoclonal antibody (1:750; Alexis Biochemicals, Vinci-Biochem, Vinci, Florence, Italy), or mouse anti-total p53 monoclonal antibody (1:500; Transduction Lab, Becton Dickinson, Milan, Italy), followed by goat anti-mouse secondary antibody conjugated to horseradish peroxidase (1:2,000; Sigma Aldrich, Milan, Italy) were used. Indeed, rabbit anti-Ser15-p53 polyclonal antibody (1:500; Biosource, Prodotti Gianni, Milan, Italy), or rabbit anti-actin polyclonal antibody (1:500; Sigma Aldrich, Milan, Italy) followed by goat anti-rabbit secondary antibody conjugated to horseradish peroxidase (1:4,000; Sigma Aldrich, Milan, Italy) were also used. Detection of proteins was performed by enhanced chemiluminescence (ECL;

Amersham Biosciences, Milan, Italy), and autoradiography. Densitometric analysis of protein bands was performed by the NIH Image 1.63 program for MacIntosh.

Total RNA Isolation, cloning, and sequencing of p53.

Total RNA was extracted as previously described (Ceruti et al., 2005). For cloning and sequencing of p53, 1 µg of RNA was treated with RQ1 RNase-free DNase (Promega, Milan, Italy) and RNA was then reverse-transcribed with Superscript II RNA H⁻ Reverse Transcriptase (200U/sample; Invitrogen, Milan, Italy). cDNAs were amplified in each PCR assay with Platinum Taq DNA polymerase (1.25 U/sample; Invitrogen, Milan, Italy) in a 25 µl reaction mixture containing 20 pmoles of 5' and 3' primers in a standard PCR buffer (50 mM KCl, 1.5 mM MgCl₂, 20 mM Tris-HCl, pH 8.4). Amplifications were performed in a GeneAmp 9700 thermal cycler (Applied Biosystems, Milan, Italy) by means of specific oligonucleotide primers. Due to the length of the p53 coding sequence (1181 bp), we performed PCR amplification by means of two pairs of primers, leading to the production of two partially overlapping amplification products, from which the full p53 sequence was reconstructed. The primers used are 1-Fw: CATGGAGGAGCCGCAGTCAG 1-Rv: 5'-TGAGGAGGGGCCAGAGGATC-3', leading to a PCR product of 576 bp, and 2-Fw: 5'-TGCCCTCAACAAGATGTTTT-3' 2-Rv: 5'-GTCTGAGTCAGGCCCTTCTG-3' leading to a PCR product of 796 bp. Amplification was performed for 35 cycles (94°C for 2 minutes, 94°C for 45 seconds, annealing at 59°C for 30 seconds, 72°C for 1 min and finally 72°C for 7 min). The PCR products were cloned into the pcDNA3.1 expression vector using the pcDNA3.1/V5-His[®]TOPO[®]TA Expression Kit (Invitrogen, Milan, Italy). Positive colonies were identified with a PCR analysis using specific oligonucleotide primers T7 (Fw: 5'-TAATACGACTCACTATAGGG-3') and BGHrev (Rw: 5'-CCTCGACTGTGCCTTCTA-

3'). The constructs were verified by sequencing using the Applied Biosystems Terminator cycle sequencing kit (PRIMM, Milan, Italy).

Statistical Analysis

All results are expressed as mean \pm s.e.m. of at least three independent experiments. Statistical significance between groups was derived from one-way ANOVA followed by the Scheffe F Test. A p value lower than 0.05 was considered significant.

RESULTS

Human astrocytoma cells are highly sensitive to a combination of proteasome inhibitors and Etoposide

Despite the lack of expression of the multidrug resistance protein (Ceruti et al., 2005), ADF cells are relatively resistant to the anti-cancer agent Eto. We exposed cultures for 24 hours to increasing Eto concentrations (Fig. 1A), and evaluated cell death by flow cytometric analysis of PI-stained nuclei. Only the highest concentrations tested (50-100 μ M) were able to induce a significant although small (never exceeding the 20%) percentage of apoptotic death. No significant signs of necrosis were detected.

We next tested the potential effects of small aldehyde peptidic proteasome inhibitors (namely, AllM, AllN and LLnV) on the survival of human astrocytoma ADF cells. These molecules represent very useful in vitro tools to understand the role of proteasome in induction and modulation of cell death (Almond and Cohen, 2002). A 24-hour exposure of ADF cells to increasing proteasome inhibitors concentrations (1-50 μ M), an experimental paradigm that has been successfully utilized in other cell lines (Dou et al., 1999; Zhu et al., 2005), had no significant effects on cell survival (Table 1).

We then decided to test whether a combination of Eto+proteasome inhibitors might modulate ADF cell survival. Fig. 1B shows the effect of various concentrations of small aldehydic peptides on the percentage of apoptotic death induced by a 18-hour incubation with Eto (continuous line). A dramatic increase in the percentage of apoptosis was detected, with a rank order of potency as follows: LLnV>AllN>AllM. LLnV was almost maximally effective at concentrations as low as 1 μ M. Based on these results, in all subsequent experiments proteasome inhibitors concentrations giving a comparable and maximal effect on Eto-induced cell death were utilized (i.e., 1 μ M, 10 μ M and 50 μ M for LLnV, AllN and AllM, respectively). The potentiating effect of the three molecules increased over time, starting from

a 12-hour incubation, and reaching a maximal effect between 18 and 24 hours (Fig. 1C). Moreover, they were effective on any Eto concentration (Fig. 1D), although the maximal results were obtained in combination with the 100 μ M Eto concentration. Interestingly, the effect of proteasome inhibitors in our experimental model is specifically directed towards Eto toxicity. In fact, no significant potentiating effect was detected when they were utilized in combination with Betulinic Acid (BetA), a mitochondriotropic anti-cancer agent which is almost ineffective in inducing ADF cell death (Ceruti et al., 2005). The percentage of apoptosis was $2.93\pm 0.6\%$ after a 72-hour incubation with 10 μ g/ml BetA, and of $7.45\pm 1.2\%$ after a concomitant exposure to BetA and AllM (50 μ M). Similar results were also obtained with the other proteasome inhibitors utilized here.

In our experimental setting, the rank order of potency of proteasome inhibitors fully overlapped with their selectivity on the proteasome complex (Dou et al., 1999). However, it is well known that these molecules could also act as inhibitors of various other intracellular enzymes, such as calpains and cathepsins (Almond and Cohen, 2002). To investigate whether inhibition of these enzymes might contribute to the detected effects, we incubated ADF cells with various chemical compounds known to act as selective inhibitors of calpains and cathepsins, and tested their ability to potentiate Eto-induced apoptosis (Table 2). No increase in the percentage of cell death was recorded when ADF cells were co-exposed to Eto and selective inhibitors of either calpains or cathepsins (i.e., E64, Calpastatin, Pepstatin or Ca-074Me; Jedinak and Maliar, 2005). Conversely, co-incubation with the natural cell-permeable proteasome inhibitor Epoxomicin (1 μ M; Schwartz et al., 2000) dramatically heightened the percentage of Eto-induced apoptosis, with a similar potency to LLnV (compare Table 2 with Fig. 1B), further confirming that the detected synergistic activity is due to proteasome inhibition.

In the experiments described above, proteasome inhibitors were added to cultures 30 minutes before Eto. In order to investigate their efficacy as a function of time, we performed a set of experiments in which these molecules were added to cultures together with, or at various times (1-7 hours) after Eto. Results shown in Fig. 2 demonstrate that the ability of proteasome inhibitors to potentiate Eto-induced cytotoxicity was progressively lost if these compounds are given after the anti-cancer agent. The limited half-life of Eto (Ciccolini et al., 2002) could contribute to the loss of synergistic activity. The less potent and less selective proteasome inhibitor ALLM is the faster in losing its activity, which is almost completely abolished after a 4-hour delayed exposure, followed by ALLN (6 hours), and LLnV (7 hours). Variability of results obtained after treating cells with Eto in combination with either ALLM or ALLN, shown by the high s.e.m. values, may be due to their lower stability with respect to LLnV (Fig. 2).

Caspase-2 and -3 are at the basis of apoptotic cell death induced by Eto and proteasome inhibitors

Human astrocytoma ADF cells bear a defective mitochondrial pathway of apoptosis (Ceruti et al., 2005), but are sensitive to caspase-2-dependent cell death (Ceruti et al., 2003). Thus, we next analyzed the caspase pathway(s) activated by Eto (alone or in combination with proteasome inhibitors), and started our evaluation from “effector” caspase-3. Fig. 3A shows the time-dependent activation of caspase-3 induced by Eto alone starting 6 hours after the beginning of incubation, and reaching a plateau after 15 hours (about 5-fold over basal activity). The concomitant incubation with proteasome inhibitors dramatically increased caspase-3 activation in a time-dependent fashion. A significant difference with respect to Eto alone was evident starting from a 10-hour incubation (before the appearance of nuclear signs of apoptosis; see Fig.1C), and the maximal activity (corresponding to 10/15-fold over basal)

was reached after 15 hours. Exposure to proteasome inhibitors alone was not sufficient to promote caspase-3 activation. As an example, a 15-hour incubation with LLnV, 1 μ M led to a caspase-3 activation of 1.76 ± 0.03 fold over basal ($p=0.24$, one way ANOVA, Scheffe F test). Similar lack of activation was detected in the presence of AllM and AllN alone. These results were confirmed by western blotting analysis with an antibody recognizing both the inactive caspase-3 pro-enzyme (detected as a 32kDa band) and its active proteolytic fragments (detected as 17-12kDa protein bands, Fig. 3B,C). Proteasome inhibitors significantly enhanced the appearance of the active caspase-3 fragments with respect to Eto alone when added 30 minutes before Eto (Fig. 3B), thus confirming the results of the colorimetric assay. Delayed exposure to proteasome inhibitors prevented this effect (Fig. 3C), in total agreement with the loss of effect on caspase-3 enzymatic activity (not shown), and with the reduced cytotoxicity of the combination Eto+proteasome inhibitors in the delayed exposure protocol (see Fig. 2).

We next examined the activation of three main upstream caspases, namely caspase-2, -9, and -8 by means of a colorimetric assay using specific substrates for each enzyme (see Methods). In cultures exposed to Eto alone, at early time points only a significant 2-fold activation of caspase-2 could be detected ($p=0.029$ for a 6-hour incubation with Eto alone with respect to corresponding Control, one way ANOVA, Scheffe F test), which remained substantially unchanged by increasing the time of exposure (Fig. 4A). Caspase-9 and -8 were slightly activated only at later time points, probably as a consequence of caspase-2 and -3 activation (see below). The concomitant exposure to Eto and proteasome inhibitors significantly changed the degree (but not the pattern) of caspase activation. In fact, caspase-2 activity was highly significantly increased (reaching a 7-fold over basal maximal activation after a 10-hour incubation in the presence of LLnV; $p=0.0001$ with respect to Control and Eto alone, one way ANOVA, Scheffe F test), whereas activation of caspase-9 and -8 was delayed,

and followed a bi-phasic pattern (with two peaks after 10 and 18 hours), never exceeding a 5- and 2-fold activation, respectively (Fig. 4A). Proteasome inhibitors alone induced no activation of caspase-2, -9, or -8. For example, in the case of a 15-hour incubation with LLnV (1 μ M) a 1.39 ± 0.01 , 1.09 ± 0.06 , and 0.85 ± 0.01 fold over basal activation was detected for caspase-2, -9, and -8, respectively. ($p=0.06$, $p=0.22$, and $p=0.08$ with respect to corresponding Control, one way ANOVA, Scheffe F test). Similar results were obtained in the presence of AllM and AllN alone.

As previously mentioned, we have demonstrated that mitochondrial depolarization is not a trigger for initiation of apoptosis in ADF cells (Ceruti et al., 2005). In fact, mitochondrial depolarization can be detected in these cells at later stages when cells are already committed to apoptosis (Ceruti et al., 2003; 2005). We thus examined changes in mitochondrial membrane potential ($\Delta\Psi_m$) in ADF cells after exposure to the pharmacological agents utilized here. Flow cytometric analysis of JC-1-stained cells showed no changes in $\Delta\Psi_m$ after exposure to Eto alone for various time periods (Fig. 4B), whereas in cells exposed to Eto in combination with proteasome inhibitors a significant enhancement of the percentage of cells with depolarized mitochondria was recorded, starting from a 15-hour incubation. At this time point, a highly significant percentage of apoptotic cells can already be detected (see Fig. 1C), suggesting the drop in $\Delta\Psi_m$ to be rather a consequence than a cause of cell death.

Caspase activation is causally related to induction of death, since the pan-caspase inhibitor zVAD-fmk (10 μ M) was able to completely abolish the appearance of the nuclear signs of apoptosis. In fact, the percentage of apoptotic death detected after a 15-hour incubation with Eto+LLnV ($46.40\pm 0.69\%$ vs $0.84\pm 0.14\%$ in Control cultures, $p<0.05$, one way ANOVA, Scheffe F test) was back to Control values in the presence of the pan-caspase inhibitor ($2.83\pm 0.20\%$, $p<0.05$ with respect to Eto+LLnV, one way ANOVA, Scheffe F test). Similar results were obtained in the presence of the other proteasome inhibitors. Surprisingly,

all the four caspases examined here seem to be equally important in triggering the executioner phase of apoptosis, leading to the appearance of nuclear fragmentation. In fact, inhibition of either one of the four caspases (obtained by utilizing the highly selective 3 μ M concentration of specific inhibitors; Ceruti et al., 2003) was able to completely prevent the appearance of nuclear signs of apoptosis induced by a 15-hour incubation with Eto+proteasome inhibitors (Fig. 5A). Thus, an auto-amplifying loop in caspase activation seems to be involved in the potentiating activity of proteasome inhibitors, since inhibition of either caspase was able to completely block the activation of all the other ones (see Fig. 5B and data not shown for caspase-8).

Human astrocytoma ADF cells express a mutated p53 isoform

The p53 tumor suppressor gene represents the most frequently mutated gene in human cancer (Soussi and Lozano, 2005), often accounting for resistance to chemotherapy. For example, it has been recently demonstrated that single nucleotide polymorphisms leading to p53 inactivation are correlated to resistance to 5-fluorouracil in pancreatic cancer (Giovannetti et al., 2006). Indeed, a higher response rate to paclitaxel+carboplatin and longer overall survival was observed in wild-type p53 patients with advanced ovarian cancer as compared to patients with mutant p53 (Gadducci et al., 2006). Due to the high level of resistance of ADF cells to anti-cancer agents, we decided to clone and sequence p53 from these cells, after checking its expression by RT-PCR analysis (data not shown).

The nucleotide sequence of p53 from ADF cells was 99% identical to that reported for human wild type p53 (GenBank accession number: NM_000546) with the exception of a single G-to-A nucleotide substitution in position 797 of the coding sequence, which was found in all the five clones analyzed. Fig. 6 shows the deduced aminoacid sequence for p53 in ADF cells and its alignment with the published human wild type p53 protein. The reported

polymorphism translates into a single aminoacid substitution at position 266 (G→E), in a region of the protein that belongs to the DNA-binding domain. This mutation has been already described in the literature as leading to an inactive p53 isoform (Chen et al., 1995; van Slooten et al., 1999).

Exposure to Eto+proteasome inhibitors modifies the subcellular localization of mutated p53

To evaluate p53 protein expression by western blotting analysis, we prepared whole-cell lysates (excluding nuclear fraction, which are discarded by a low speed initial centrifugation; see Methods) from Control cultures or from cells exposed for various time periods to either Eto alone or in combination with proteasome inhibitors. Immunodetection of actin expression was used as an internal control for correct protein loading in the gel. Interestingly, p53 is highly expressed in Control ADF cultures, suggesting that the reported mutation might have increased its stability (see Discussion). A significant and time-dependent reduction of the p53 protein band was detected upon exposure to Eto+LLnV (Fig. 7A, B). Under this condition, reduction of p53 was due to a post-translational event since semiquantitative RT-PCR analysis showed identical p53 mRNA levels (data not shown). Cultures exposed to LLnV alone showed no differences in the p53 protein band with respect to Control cultures (Fig. 7D). Retardation of exposure to LLnV (e.g., addition of the inhibitor 7 hours after Eto) was able to completely prevent p53 reduction (Fig. 7A, B), in line with the results obtained on caspase activation and induction of apoptosis with the delayed protocol (see Figs. 2, 3C). Caspase inhibitors were not able to prevent p53 reduction (data not shown), suggesting that this event is upstream of the activation of the caspase cascade.

We next examined the subcellular localization of p53 protein. Western blotting analysis clearly showed that, in Control cultures or in cells exposed to either Eto or

proteasome inhibitors alone, mutated p53 was distributed between the cytosolic and the nuclear fractions (Fig. 7C, D), whereas nuclear localization became predominant in the presence of Eto+proteasome inhibitors (Fig. 7C).

To test whether re-localization of the p53 protein towards the nuclear compartment might have contributed to the potentiation of apoptotic cell death, we exposed cells to Eto+LLnV for 18 hours in the presence of 25 μ M pifithrin- α (PFT- α), known to inhibit the transcriptional events downstream of p53 (Seth et al., 2005). Under this experimental protocol, in cells exposed to Eto plus proteasome inhibitors, the percentage of apoptosis was partially but significantly reduced to 38%, with respect to 52% in the absence of pifithrin- α (data not shown).

Phosphorylation of p53 on Ser-15 is not sufficient to promote ADF cell apoptosis

It has been proposed that post-translation modifications, such as serine and threonine phosphorylation, are fundamental for p53 to exert its pro-apoptotic effects. In particular, phospho-Ser15-p53 has been implicated in several paradigms of apoptosis (Wu, 2004). To test whether this could be the case also in our experimental model, we have performed western blotting analysis by means of a specific anti phospho-Ser15-p53 protein. In whole cell lysates, no phosphorylation on Ser15 of the p53 protein was detected in Control cultures, whereas after exposure to Eto or to proteasome inhibitors alone, a specific band could be observed (Fig. 8A, D). The concomitant exposure to Eto and proteasome inhibitors significantly reduced the amount of phospho-Ser15-p53 over time (Fig. 8A, B). This was not due to a re-localization of the phosphorylated protein, since a low percentage of the total p53 nuclear protein was found phosphorylated ($30.8\pm 0.9\%$ in the Eto+LLnV samples compared to $87.1\pm 3.2\%$ in the presence of Eto alone; Fig. 8C), thus confirming that an actual reduction in the total amount of phosphorylated p53 was present under apoptotic conditions.

DISCUSSION

The search for new anti-cancer drug combinations and/or strategies has recently hastened, and the use of cancer cell lines bearing specific mutations of cell death pathways has greatly helped verifying in vitro the ability of chemotherapeutic agents to overcome chemoresistance. In this respect, proteasome inhibitors have been shown to activate various anti-neoplastic mechanisms, including pathways controlling apoptosis (Mendoza et al., 2005), and may therefore represent a new and effective class of anti-cancer agents. Our results show that small aldehydic peptides acting as proteasome inhibitors can be effectively utilized to restore sensitivity of human astrocytoma cells to Eto-induced apoptosis, by inducing the relocalization of p53 to the nuclear compartment and a highly significant caspase activation.

The human astrocytoma cell line (ADF cells) utilized by us in this and previous studies bears a defective mitochondrial pathway of apoptosis (Ceruti et al., 2005), as well as a mutated p53 isoform (the present study). The inability to activate the intrinsic pathway of apoptosis is due to the presence of a mutation in the caspase-9 protein, and to the expression of a dominant negative isoform of the enzyme, alterations that probably prevent apoptosome formation (Ceruti et al., 2005). Thus, due to the presence of multiple genetic alterations, ADF cells are resistant to “mitochondriotropic” agents (such as Betulinic Acid or 2-deoxy-ribose; Ceruti et al., 2005). Moreover, the impaired functions of p53 and caspase-9 might also contribute to resistance to proteasome inhibitors (when utilized alone), and to Eto (see Table 1 and Fig. 1).

Interestingly, we have demonstrated that ADF cells retain the ability to undertake an apoptotic program when exposed to caspase-2 activating agents (such as Cladribine; Ceruti et al., 2003), and a key role for this enzyme in induction of apoptosis in our experimental model is further strengthened by the present study. In fact, exposure to Eto alone led to a significant, although modest, activation of caspase-2 and caspase-3 (Figs. 3,4A), with a consequent very

low percentage of apoptotic cell death (Fig. 1A). Instead, highly significant apoptosis can be obtained after exposure to Eto+proteasome inhibitors, when a highly significant activation of caspase-2 and -3 is achieved followed by a delayed activation of caspase-8 and -9 (Fig. 4A). This suggests that, despite the inability to assemble the apoptosome complex (see above), caspase-9 can still be activated by direct cleavage exerted by other caspases. In the terminal executioner phase of the apoptotic program, all these four members of the family become equally important, also contributing to each other's recruitment (Fig. 5A,B).

A similar redundant auto-amplifying pattern of caspase activation has been described in cell free extracts from Jurkat cells exposed to granzyme B, where caspase-8, -3, -10, and -7 were initially activated in parallel, and a second caspase-3-dependent wave of enzymatic activation included caspase-2, -9, and -6 (Adrain et al., 2005). Therefore, it can be hypothesized that, in cancer cells where the "classical" pathways of death cannot be recruited, an atypical auto-amplifying loop of caspase activation still retains the ability to complete an effective apoptotic program.

Several mechanisms may be at the basis of the sensitizing effect of proteasome inhibitors on Eto-induced toxicity. The fact that proteasome inhibitors are not effective per se suggests that they do not interfere with a constitutive survival pathway, which might have contributed to the malignant transformation and growth advantage of ADF cells, but rather act towards protective mechanism(s) that are activated in response to Eto. It is also worth noting that proteasome inhibitors are not able to prevent ADF cell resistance to other cytotoxic agents, such as BetA, suggesting a selectivity of action on specific intracellular pathways that are activated by some chemotherapeutic agents (e.g., Eto) but not by others.

In this respect, it has been demonstrated that exposure of cancer cell to chemotherapy may activate the transcription factor NF- κ B, through proteasome-mediated degradation of its inhibitor I κ B α (Leverkus et al., 2003; Richardson et al., 2005). NF- κ B initiates a number of

survival pathways, including an increased synthesis of Inhibitors of Apoptosis Proteins (IAPs; Richardson et al., 2005). These proteins inhibit activation of upstream caspases, therefore limiting the extent of apoptotic death. Interestingly, it has been also demonstrated that XIAP can exert an inhibitory effect on downstream caspase-3 by addressing its degradation by the proteasome complex, leading to the appearance of partially cleaved caspase-3 fragments, with very low catalytic activity (Leverkus et al., 2003). This scenario could be hypothesized also in our experimental model, in which incubation with Eto is not sufficient to trigger a complete, and therefore efficacious, caspase-3 cleavage that can be only achieved after a pre-incubation with proteasome inhibitors (Fig. 3). Delaying incubation with LLnV progressively reduced its ability to promote full caspase-3 maturation (Fig. 3C), and to potentiate induction of cell death (Fig. 2). This suggests that a very narrow time window exists to overcome the anti-apoptotic strategies activated by the tumor cell, which otherwise become predominant, allowing cells to escape from death.

Our data also suggest a role for p53 in induction of cell death by Eto+proteasome inhibitors, despite the presence of a G-to-A mutation in position 797, which translates into the substitution of a Glycine with a Glutamic Acid residue at position 266 (Fig. 6) belonging to the DNA binding domain of the protein (van Slooten et al., 1999). This mutation has been already described in human tumors (for a complete list, see <http://p53.free.fr>), including astrocytomas (Chen et al., 1995). ADF-expressed mutated p53 is characterized by a higher stability with respect to wild-type protein, as demonstrated by its expression under control conditions (Fig. 7), suggesting its inability to promote cell death or to block the progression of the cell cycle. In fact, the protein isoform bearing the G797-to-A mutation has been shown transcriptionally inactive in other experimental models (van Slooten et al., 1999). On the other hand, it has been also hypothesized that mutated p53 isoforms might not only loss their trans-

activating functions, but could also gain pro-survival functions thus contributing to the propagation and survival of cancer cells (Blagosklonny, 2000).

However, it has recently become clear that p53 mutants may still retain the ability to trans-activate selected gene targets within the cell (Kim and Deppert, 2004), and to act as trans-repressor by competing with transcription factors for coactivators, and this latter activity does not require DNA binding (Blagosklonny, 2000). We speculate that these mechanisms may be at the basis of ADF cell death in the presence of Eto+proteasome inhibitors, where a partial although significant protection was exerted by pifithrin- α , known to antagonize p53 transcriptional activity (Gudkov and Komarova, 2005). In parallel, through its trans-repressor ability p53 might, for instance, counteract the protective pathways that are activated in response to Eto. To further support this hypothesis, the full nuclear localization of mutated p53 seems to be important in mediating the effects of proteasome inhibitors on Eto-toxicity, since it is progressively lost in parallel to a reduction of cell death after a delayed exposure to these agents (Figs. 2,3,7). It can be hypothesized that Eto exposure also enhances proteasome-mediated degradation of some key proteins involved in p53 nuclear localization (such as importins; Liang and Clarke, 2001; Kodiha et al., 2004), and that only after proteasome inhibition can p53 contribute to induction of apoptosis by fully re-localizing to the nuclear compartment.

Phosphorylation and acetylation of p53 are the most frequent post-translational modifications involved in its tumor suppressor activity, which can occur on various aminoacidic residues (Bode and Dong, 2004). Here, we have investigated the possible role of Ser15 phosphorylation, which has been implicated in several paradigms of cell death, but data suggest that it is not important in our experimental model. In fact, despite the ability of Eto and proteasome inhibitors when utilized alone to induce p53-Ser15 phosphorylation (Fig. 8),

this event is not sufficient to trigger the apoptotic program which is only seen after p53 nuclear re-localization (see above).

The combination of Eto+proteasome inhibitors has been tested on various in vitro models of cancer cell lines, leading to a variety of results. An additive effect in reducing cell survival has been observed in T-cell lymphomas (Nasr et al., 2005), whereas proteasome inhibition was able to circumvent resistance to Eto in cancer cells exposed to glucose starvation (Ogiso et al., 2000). It is worth noting that no restoration of Eto-induced toxicity was achieved by inhibiting proteasome functions in chemoresistant Bcl-2 expressing Jurkat cells, which instead became highly sensitive to TRAIL-induced death (Nencioni et al., 2005). Together with the present data, these results further confirm that the outcome of a given pharmacological treatment or therapeutic protocol strongly depends upon the molecular and biochemical equipment of cancer cells. Therefore, the anti-cancer potential of any given therapeutic protocol should be investigated by means of experimental models bearing different defective pathways of death. Alternatively, personalized anti-cancer therapies could be designed, by testing in vitro the sensitivity of biotically drawn cells to different pharmacological protocols. Based on our results obtained in human astrocytoma ADF cells, we speculate that, when used in combination with Eto, proteasome inhibitors might successfully kill cells expressing mutated p53 or dominant negative caspase-9 isoforms.

ACKNOWLEDGEMENTS

Authors are deeply grateful to Dr. Davide Lecca for useful discussion on the strategy for isolation and cloning of p53.

REFERENCES

Adams J and Kauffman M (2004) Development of the proteasome inhibitor Velcade (Bortezomib). *Cancer Invest* **22**:304-311.

Adrain C, Murphy BM and Martin SJ (2005) Molecular ordering of the caspase activation cascade initiated by the cytotoxic T lymphocyte/natural killer (CTL/NK) protease granzyme B. *J Biol Chem* **280**:4663-4673.

Almond JB and Cohen GM (2002) The proteasome: a novel target for cancer chemotherapy. *Leukemia* **16**:433-443.

Blagosklonny MV (2000) p53 from complexity to simplicity: mutant p53 stabilization, gain-of-function, and dominant-negative effect. *FASEB J* **14**:1901-1907.

Bode AM and Dong Z (2004) Post-translational modification of p53 in tumorigenesis. *Nat Rev Cancer* **4**:793-805.

Ceruti S, Barbieri D, Veronese E, Cattabeni F, Cossarizza A, Giammarioli AM, Malorni W, Franceschi C and Abbracchio MP (1997) Different pathways of apoptosis revealed by 2-chloro-adenosine and deoxy-D-ribose in mammalian astroglial cells. *J Neurosci Res* **47**:372-383.

Ceruti S, Franceschi C, Barbieri D, Malorni W, Camurri A, Giammarioli AM, Ambrosini A, Racagni G, Cattabeni F and Abbracchio MP (2000) Apoptosis induced by 2-chloro-adenosine

and 2-chloro-2'-deoxy-adenosine in a human astrocytoma cell line: differential mechanisms and possible clinical relevance. *J Neurosci Res* **60**:388-400.

Ceruti S, Beltrami E, Matarrese P, Mazzola A, Cattabeni F, Malorni W and Abbracchio MP (2003). A key role for caspase-2 and caspase-3 in the apoptosis induced by 2-chloro-2'-deoxy-adenosine (cladribine) and 2-chloro-adenosine in human astrocytoma cells. *Mol Pharmacol* **63**:1437-1447.

Ceruti S, Mazzola A and Abbracchio MP (2005) Resistance of human astrocytoma cells to apoptosis induced by mitochondria-damaging agents: possible implications for anticancer therapy. *J Pharmacol Exp Ther* **314**:825-837.

Chen P, Iavarone A, Fick J, Edwards M, Prados M and Israel MA (1995) Constitutional p53 mutations associated with brain tumors in young adults. *Cancer Genet Cytogenet* **82**:106-115.

Ciccolini J, Monjanel-Mouterde S, Bun SS, Blanc C, Duffaud F, Favre R and Durand A (2002) Population pharmacokinetics of etoposide: application to therapeutic drug monitoring. *Ther Drug Monit* **24**:709-714.

Denlinger CE, Rundall BK, Keller MD and Jones DR (2004) Proteasome inhibition sensitizes non-small-cell lung cancer to gemcitabine-induced apoptosis. *Ann Thorac Surg* **78**:1207-1214.

Dou QP, McGuire TF, Peng Y and An B (1999) Proteasome inhibition leads to significant reduction of Bcr-Abl expression and subsequent induction of apoptosis in K562 human chronic myelogenous leukemia cells. *J Pharmacol Exp Ther* **289**:781-790.

Fortugno P, Wall NR, Giodini A, O'Connor DS, Plescia J, Padgett KM, Tognin S, Marchisio PC and Altieri DC (2002) Survivin exists in immunochemically distinct subcellular pools and is involved in spindle microtubule function. *J Cell Sci* **115**:575-585.

Gadducci A, Di Cristofano C, Zavaglia M, Giusti L, Menicagli M, Cosio S, Naccarato AG, Genazzani AR, Bevilacqua G and Cavazzana AO (2006) p53 gene status in patients with advanced serous epithelial ovarian cancer in relation to response to paclitaxel- plus platinum-based chemotherapy and long-term clinical outcome. *Anticancer Res* **26**:687-693.

Giovannetti E, Mev V, Nannizzi S, Pasqualetti G, Del Tacca M and Danesi R (2006) Pharmacogenetics of anticancer drug sensitivity in pancreatic cancer. *Mol Cancer Ther* **5**: 1387-1395.

Gudkov AV and Komarova EA (2005) Prospective therapeutic applications of p53 inhibitors. *Biochem Biophys Res Commun* **331**:726-736.

Henderson CJ, Aleo E, Fontanini A, Maestro R, Paroni G and Brancolini C (2005) Caspase activation and apoptosis in response to proteasome inhibitors. *Cell Death Differ* **12**:1240-1254.

Jäättelä M (2004) Multiple cell death pathways as regulators of tumour initiation and progression. *Oncogene* **23**:2746-2756.

Jedinak A and Maliar T (2005). Inhibitors of proteases as anticancer drugs. *Neoplasma* **52**:185-192.

Kim E and Deppert W (2004) Transcriptional activities of mutant p53: when mutations are more than a loss. *J Cell Biochem* **93**:878-886.

Kodiha M, Chu A, Matusiewicz N and Stochaj U (2004) Multiple mechanisms promote the inhibition of classical nuclear import upon exposure to severe oxidative stress. *Cell Death Differ* **11**:862-874.

Korones DN, Benita-Weiss M, Coyle TE, Mechtler L, Bushunow P, Evans B, Reardon DA, Quinn JA and Friedman H (2003) Phase I study of Temozolomide and escalating doses of oral etoposide for adults with recurrent malignant glioma. *Cancer* **97**:1963-1968.

Leverkus M, Sprick MR, Wachter T, Mengling T, Baumann B, Serfling E, Brocker EB, Goebeler M, Neumann M and Walczak H (2003) Proteasome inhibition results in TRAIL sensitization of primary keratinocytes by removing the resistance-mediating block of effector caspase maturation. *Mol Cell Biol* **23**:777-790.

Liang S-H and Clarke MF (2001) Regulation of p53 localization. *Eur J Biochem* **268**:2779-2783.

Mendoza FJ, Espino PS, Cann KL, Bristow N, McCrea K and Los M (2005). Anti-tumor chemotherapy utilizing peptide-based approaches – apoptotic pathways, kinases, and proteasome as targets. *Arch Immunol Ther Exp* **53**:47-60.

Nasr R, El-Sabban ME, Karam J-A, Dbaibo G, Kfoury Y, Arnulf B, Lepelletier Y, Bex F, de Thé H, Hermine O and Bazarbachi A (2005) Efficacy and mechanism of action of the proteasome inhibitor PS-341 in T-cell lymphomas and HTLV-1 associated adult T-cell leukemia/lymphoma. *Oncogene* **24**:419-430.

Nencioni A, Wille L, Dal Bello G, Boy D, Cirmena G, Wesselborg S, Belka C, Brossart P, Patrone F and Ballestrero A (2005) Cooperative cytotoxicity of proteasome inhibitors and tumor necrosis factor-related apoptosis-inducing ligand in chemoresistant Bcl-2 overexpressing cells. *Clin Cancer Res* **11**:4259-4265.

Ogiso Y, Tomida A, Lei S, Omura S and Tsuruo T (2000) Proteasome inhibition circumvents solid tumor resistance to topoisomerase II-directed drugs. *Cancer Res* **60**:2429-2434.

Richardson PG, Mitsiades C, Hideshima T and Anderson KC (2005) Proteasome inhibition in the treatment of cancer. *Cell Cycle* **4**:290-296.

Schwarz K, de Giuli R, Schmidtke G, Kostka S, van den Broek M, Bo Kim K, Crews CM, Kraft R and Groettrup M (2000) The selective proteasome inhibitors Lactacystin and Epoxomicin can be used to either up- or down-regulate antigen presentation in nontoxic doses. *J Immunol* **164**:6147-6157.

Seth R, Yang C, Kaushal V, Shah SV and Kaushal GP (2005) p53-dependent caspase-2 activation in mitochondrial release of apoptosis-inducing factor and its role in renal tubular epithelial cell injury. *J Biol Chem* **280**:31230-31239.

Soussi T and Lozano G (2005) p53 mutation heterogeneity in cancer. *Biochem Biophys Res Commun* **331**:834-842.

van Slooten HJ, van De Vijver MJ, Borresen AL, Eyfjord JE, Valgardsdottir R, Scherneck S, Nesland JM, Devilee P, Cornelisse CJ and van Dierendonck JH (1999) Mutations in exons 5-8 of the p53 gene, independent of their type and location, are associated with increased apoptosis and mitosis in invasive breast carcinoma. *J Pathol* **189**:504-513.

Watanabe K, Kanaya H, Fujiamia Y and Kim P (2002) Combination chemotherapy using carboplatin (JM-8) and etoposide (JET Therapy) for recurrent malignant gliomas: a phase II study. *Acta Neurochir* **144**:1265-1270.

Wu GS (2004) The functional interactions between the p53 and MAPK signaling pathways. *Cancer Biol Ther* **3**:156-161.

Zhu H, Zhang L, Dong F, Guo W, Wu S, Teraishi F, Davis JJ, Chiao PJ and Fang B (2005) Bik/NBK accumulation correlates with apoptosis-induction by bortezomib (PS-341, Velcade) and other proteasome inhibitors. *Oncogene* **24**:4993-4999.

FOOTNOTES

This work was partially supported by the Italian Ministero dell'Istruzione, dell'Università e della Ricerca (MIUR), Fondo per gli Investimenti per la Ricerca di Base (FIRB) on “Adenosine Analogs as Potential Anti-Neoplastic Agents in Nonhematological Tumors: In Vitro Effects on Cell Cycle Progression and Induction of Apoptosis in Human Cancerous Cells” (to S.C. and M.P.A.).

Address reprints request to: Prof. Maria P. Abbraccio-Department of Pharmacological Sciences, University of Milan-Via Balzaretto, 9-20133 Milan ITALY. E-mail: mariapia.abbraccio@unimi.it

LEGENDS FOR FIGURES

Figure 1. Small aldehydic peptides potentiate Eto-induced apoptosis in human astrocytoma ADF cells. Evaluation of the percentage of cell death after a 24-hour exposure to various Eto concentrations alone (Panel A), or in the presence of selected concentrations of small aldehydic peptides (Panel D). Concentration- (Panel B; 18-hour incubation), and time- (Panel C) dependent potentiation of Eto cytotoxicity by small aldehydic peptides. Results represent the mean \pm s.e.m. of at least 3 independent experiments. * p <0.05 with respect to Control, and § p <0.05 with respect to Eto alone; one way ANOVA (Scheffe F test).

Figure 2. Proteasome inhibitors progressively lose their potentiating activity on apoptosis when added to cultures after Eto. ADF cells were grown in the presence of either Eto alone or in combination with proteasome inhibitors, which were added to cultures at various time points after Eto. After 24 total hours in culture, the percentage of apoptosis was evaluated by flow cytometric analysis of PI-stained nuclei. * p <0.05 with respect to corresponding Control, and § p <0.05 with respect to Eto alone; one way ANOVA (Scheffe F test).

Figure 3. Proteasome inhibitors potentiate Eto-induced caspase-3 activation. Panel A. Cells were grown in the presence of the indicated drugs for various time periods (X-axis). At the end of incubation, caspase-3 activation was evaluated by means of a colorimetric technique (see Methods). Results are expressed as fold over basal activation, and represent the mean \pm s.e.m. of at least 5 independent experiments run in triplicate. * p <0.05 with respect to corresponding Control, and § p <0.05 with respect to Eto alone; one way ANOVA (Scheffe F test). Panel B and C. Western blotting analysis of caspase-3 activation. Cells were grown for 15 hours in the presence of the indicated drugs (B). At the end of the incubation period, western blotting analysis was performed as described in Methods. The low molecular weight

bands, which are significantly detectable only after exposure to Eto+proteasome inhibitors, represent the active fragments of the enzyme. Panel C. LLnV loses its ability to increase caspase-3 activation when added 7 hours after Eto. Western blotting analysis of cells exposed for 10 hours to Eto alone or in combination with the proteasome inhibitor LLnV, added to cultures either 30 minutes before or 7 hour after Eto. Similar results have been obtained in the presence of Eto+AllM or AllN (data not shown). In both Panels B and C actin immunoreactivity is shown to check for equal protein loading in the gel.

Figure 4. Panel A. Time-dependent activation of caspase-2, -9, and -8 by Eto, and potentiation by proteasome inhibitors. Cells were grown in the presence of the indicated drugs for various time periods (X-axis), and caspase activation was then evaluated by means of a colorimetric technique (see Methods). Results are expressed as fold over basal activation, and represent the mean±s.e.m. of at least 5 independent experiments run in triplicate. Panel B. A significant drop in mitochondrial membrane potential can be detected only starting from a 15-hour incubation with Eto+proteasome inhibitors. Cells were grown in the presence of the indicated drugs for various time periods (X-axis), and the mitochondrial membrane potential was then evaluated by flow cytometry with the JC-1 dye (Ceruti et al., 2005). Results represent the percentage of cells showing mitochondrial depolarization, expressed as the mean±s.e.m. of three independent experiments. * $p < 0.05$ with respect to corresponding Control, and § $p < 0.05$ with respect to Eto alone; one way ANOVA (Scheffe F test).

Figure 5. Panel A. Selective caspase inhibitors completely prevent the appearance of nuclear signs of apoptosis induced by Eto+proteasome inhibitors. Cells were grown for 15 hours in the presence of the indicated drug combinations, and the percentage of apoptotic cells was then evaluated by flow cytometric analysis of PI-stained nuclei. Results represent the

mean±s.e.m. of at least three independent experiments. Panel B. A concomitant activation of caspase-3, -9, and -2 can be detected after a 10-hour incubation with Eto+proteasome inhibitors. Cells were grown in the presence of the indicated drug combinations, and at the end of the incubation period caspase activation was evaluated by means of a colorimetric technique (see Methods). Results are expressed as fold over basal activation, and represent the mean±s.e.m. of at least 3 independent experiments run in triplicate. *p<0.05 with respect to Control; #p<0.05 with respect to Control and Eto alone; §p<0.05 with respect to Eto alone, and ^p<0.05 with respect to Control and to the corresponding combination of Eto+proteasome inhibitor; one way ANOVA (Scheffe F test).

Figure 6. Human astrocytoma ADF cells express a mutated p53 isoform. Predicted amino acid sequence obtained from cloning and sequencing of the p53 gene from human astrocytoma ADF cells, and alignment with the corresponding human wild-type protein (GenBank accession number NM_000546). A point mutation in the 797 position (G→A) was detected in every tested clone, leading to the substitution in the 266 position, belonging to the DNA binding domain of the protein (spanning from aa. 101 to aa 306; Bode and Dong, 2004), of a glycine (G) with a glutamic acid (E) residue.

Figure 7. The combination of Eto+LLnV induces migration of the p53 protein from the cytosolic to the nuclear fraction. Panel A. Cells were grown in the absence (Control; C) or presence of Eto alone or in combination with LLnV for the indicated time periods. In experiments shown in the upper part of the figure, LLnV was added 30 minutes before Eto; in the lower part of the figure, LLnV was added 7 hours after Eto, as indicated. For each experimental condition, actin expression was evaluated to check for correct loading of gel. Panel B. Densitometric analysis of p53 expression, corrected for the corresponding actin

band, and expressed as % of Control \pm s.e.m. Results represent the mean of at least three independent experiments. * p <0.05 with respect to Control and Eto alone, one way ANOVA (Scheffe F test). Panel C. Exposure to Eto+LLnV increases the nuclear localization of p53. Cells were grown for 15 hours in the absence (Control; C) or presence of Eto alone or in combination with LLnV (added 30 minutes before Eto). Cells were then collected, and the cytosolic, and nuclear compartments were separated as described in Methods. Similar results have been obtained also by combining Eto with AllM, 50 μ M or AllN, 10 μ M (data not shown). Panel D. LLnV has no effect “per se” on the subcellular localization of the p53 protein. Protein extraction, subcellular localization, and western blotting analysis of p53 and actin were performed as described above on cultures exposed for 15 hours to LLnV, 1 μ M alone. Upper western blots refer to whole-cell extracts, lower western blots to cytosol and nuclei, as indicated. Similar results were obtained in the presence of AllM, and AllN. For each experimental condition, western blotting analysis of total p53 was performed after stripping and re-probing nitrocellulose membranes that have been previously exposed to an anti-phospho-Ser15-p53 antibody, as indicated in Methods (see also Legend to Fig. 8).

Figure 8. Phosphorylation of p53 on Ser15 does not play a role in Eto+proteasome inhibitors-induced cell death. Nitrocellulose membranes shown in Panels A, C, and D are the same filters shown in Fig. 7 that have been exposed to an anti-phospho-Ser15 antibody, and then re-probed to detect total p53 (see Legend to Fig. 7 for details). Panel B. Densitometric analysis of phospho-Ser15 p53, corrected for the corresponding actin band, and expressed as % of Eto alone \pm s.e.m. Results represent the mean of at least three independent experiments. * p <0.05 with respect to Eto alone, one way ANOVA (Scheffe F test).

Table 1. Proteasome inhibitors have no effect “per se” on ADF cell survival

| % of apoptotic death (mean±S.E.) | | | |
|----------------------------------|-----------|-------------------------|-----------|
| | AllM | AllN | LLnV |
| 1 μM | | 0.53±0.01 | 4.50±1.67 |
| 10 μM | | 3.34±0.43 | 5.95±1.82 |
| 50 μM | 0.53±0.31 | 10.49±3.73 ^a | 5.47±1.08 |

Human astrocytoma ADF cells were grown for 24 hours in the presence of various concentrations of aldehyde peptidic proteasome inhibitors. At the end of the incubation period, the percentage of apoptosis was evaluated by flow cytometry after PI staining of nuclei. % of death in Control cultures was 1.2±0.09. Results represent the mean±S.E.M. of three to five independent experiments. ^ap<0.05 with respect to corresponding Control, one way ANOVA (Scheffe F test)

Table 2. Calpain and cathepsin inhibitors are ineffective, whereas the natural proteasome inhibitor Epoxomicin is highly effective in potentiating Eto-induced cell death in ADF cells.

| | % of apoptotic death (mean±s.e.m.) |
|---------------------|--|
| Control (18 hours) | 1.18±0.33 |
| Eto, 100 μM | 9.53±0.95 ^a |
| +E64, 50 μM | 8.82±0.67 ^a |
| +Pepstatin, 10 μM | 7.96±1.96 ^a |
| +Ca-074Me, 50 μM | 9.65±0.35 ^a |
| +Epoxomicin, 1 μM | 48.39±0.87 ^b |
| Control (24 hours) | 1.65±0.75 |
| Eto, 100 μM | 16.03±5.02 ^a |
| +Calpastatin, 10 μM | 16.84±5.34 ^a |

Human astrocytoma ADF cells were grown under Control condition or in the presence of either Eto alone or in combination with various pharmacological agents. At the end of the incubation period, the percentage of apoptotic death was evaluated by flow cytometric analysis of PI-stained nuclei. Epoxomicin was not toxic per se up to a 10 μM concentration (percentage of cell death: 3.35±0.74%, p=0.08 with respect to Control, one way ANOVA, Scheffe F test). Results represent the mean±S.E.M. of three independent experiments. ^ap<0.05 with respect to corresponding Control, ^bp<0.05 with respect to corresponding Control and Eto alone, one way ANOVA (Scheffe F test).

Figure 1

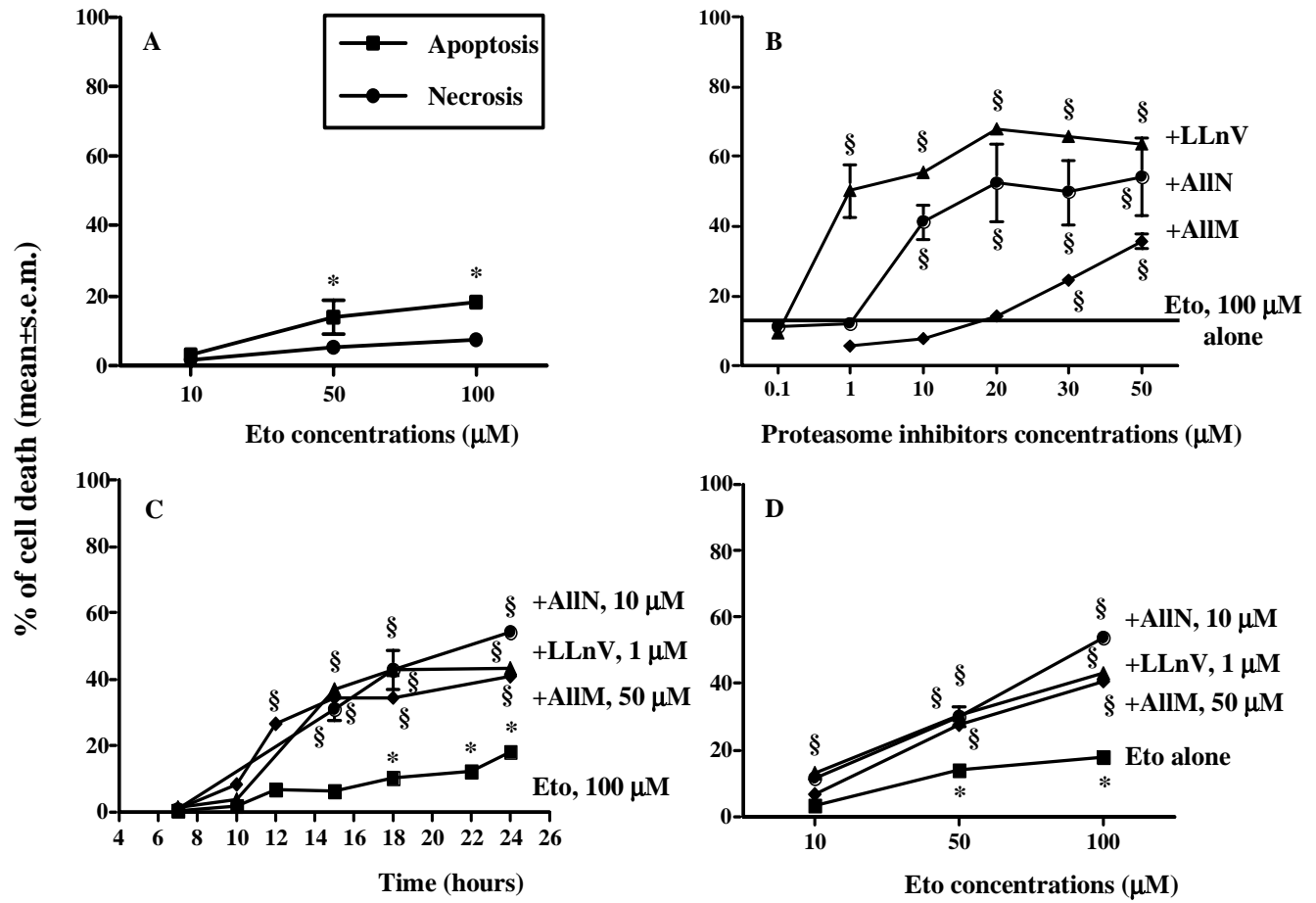


Figure 2

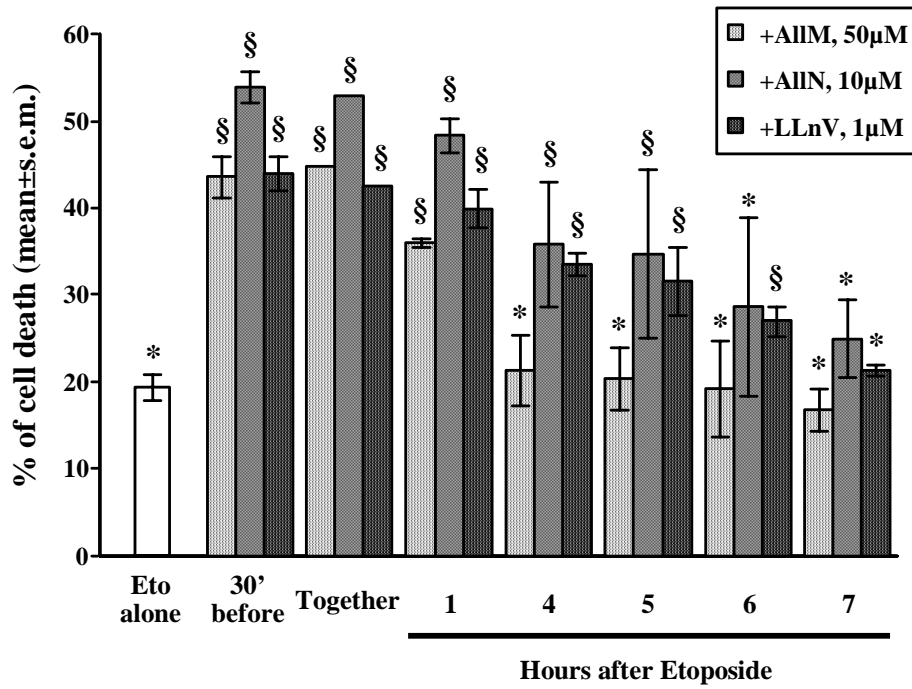


Figure 3

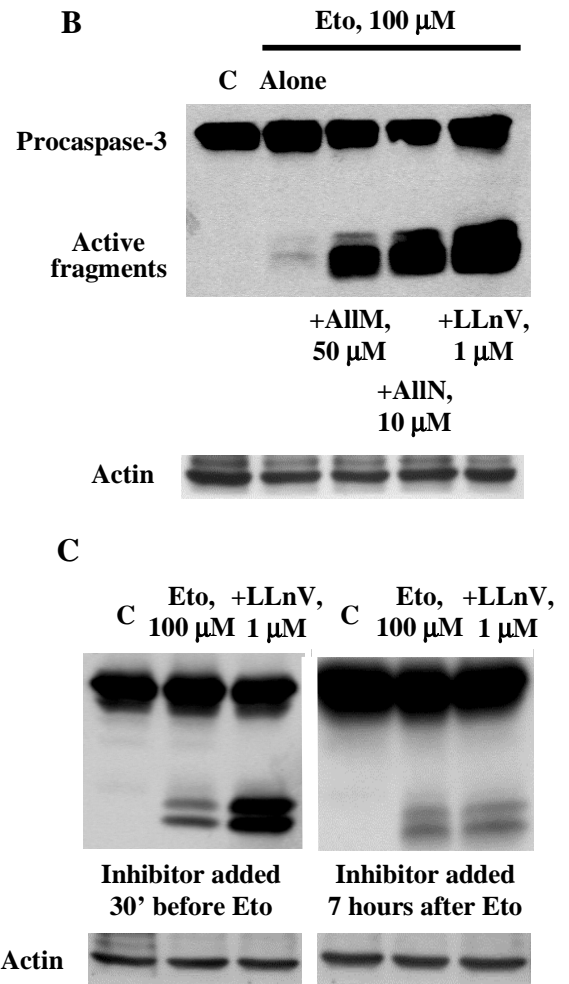
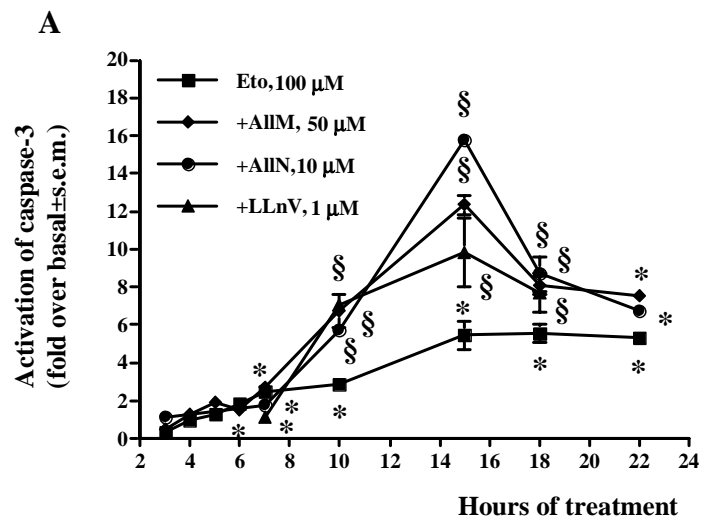
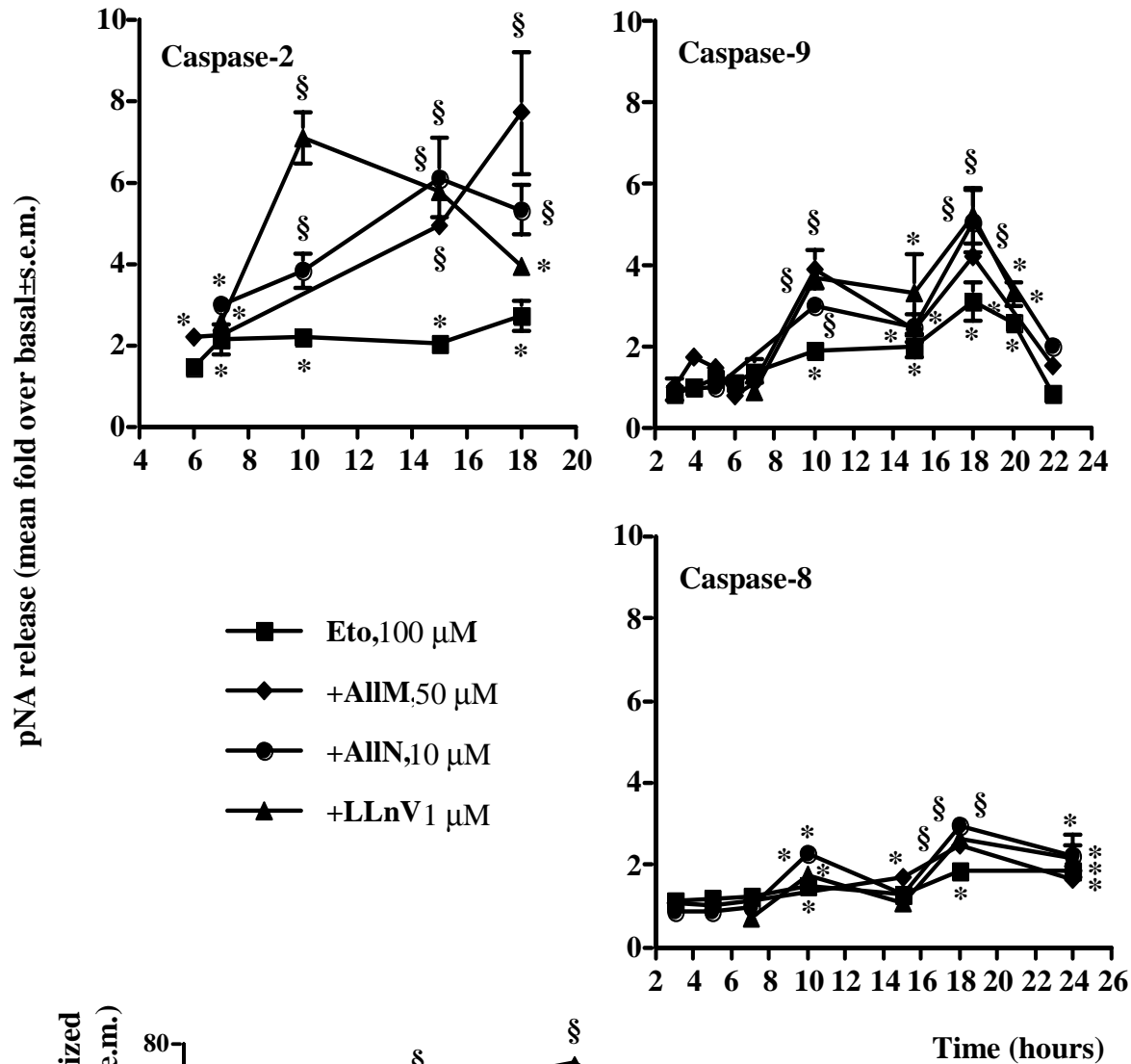


Figure 4

A



B

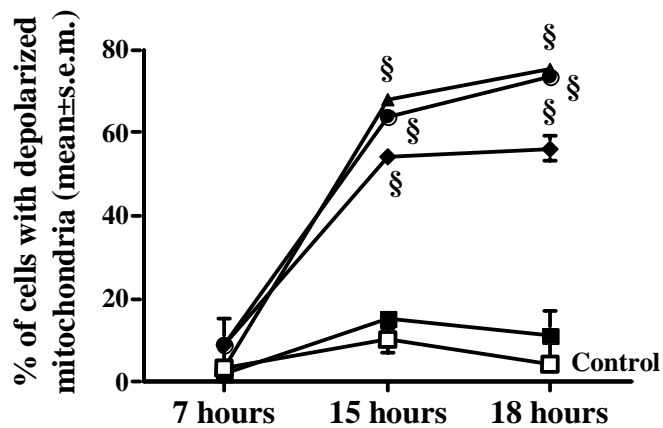


Figure 5

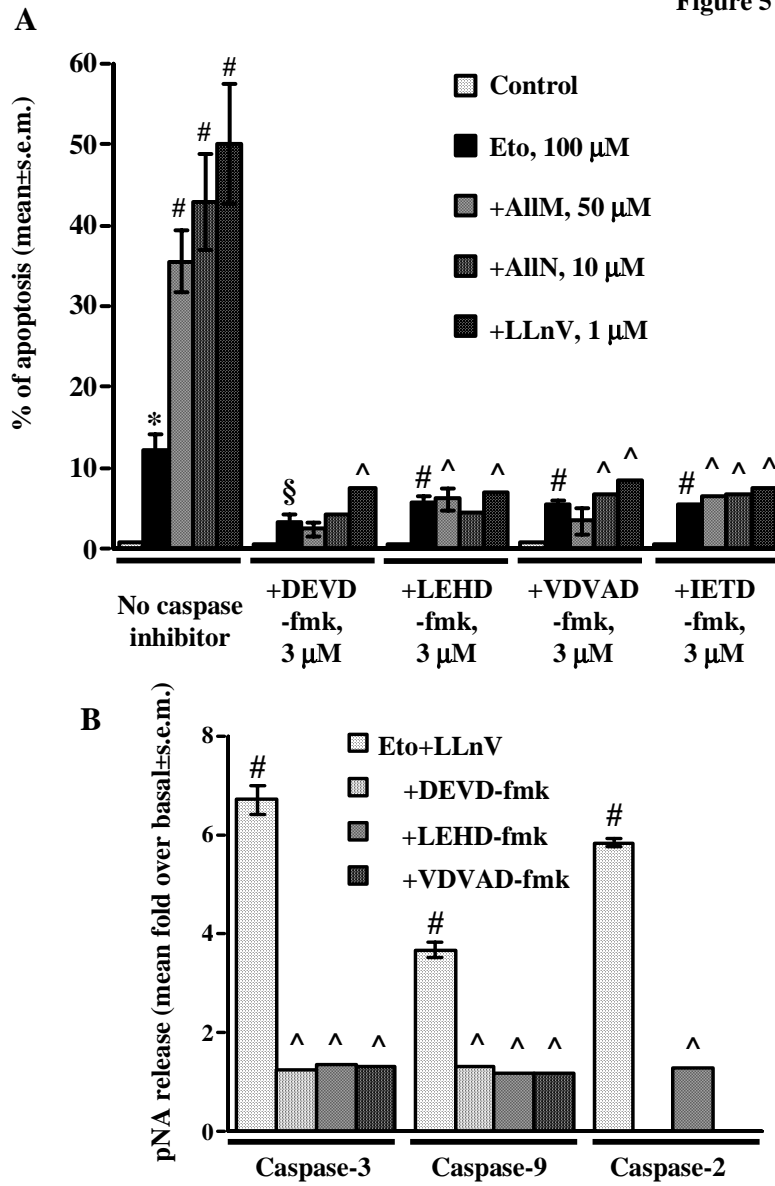


Figure 6

| | |
|----------------|---|
| h p53 | 1-MEEPQSDPSVEPPLSQETFSDLWKLPE NN VLSPLPSQAMDDLMLSPDDIEQW |
| ADF p53 | 1-MEEPQSDPSVEPPLSQETFSDLWKLPE NN VLSPLPSQAMDDLMLSPDDIEQW |
| h p53 | FTEDPGPEAPRMPEAAPRVAPAPAAPTPAAPAPASWP LSSSVPSQKTYQGSY |
| ADF p53 | FTEDPGPEAPRMPEAAPRVAPAPAAPTPAAPAPAPSWPLSSSVPSQKTYQGSY |
| h p53 | GFRLGFLHSGTAKSVTCTYSPALNKMFCQLAKTCVPQLWVDS TPPP GTRVRA |
| ADF p53 | GFRLGFLHSGTAKSVTCTYSPALNKMFCQLAKTCVPQLWVDSTPPP GTRVRA |
| h p53 | MAIYKQSQHMTEV VRRCPHHERCSDSDGLAPPQHLIRVEGNLRVEYLDDRNT |
| ADF p53 | MAIYKQSQHMTEV VRRCPHHERCSDSDGLAPPQHLIRVEGNLRVEYLDDRNT |
| h p53 | FRHSVVVPYEPPEVGS DCTTIHYNMCMNSSCMGGMNRRPILTIITLEDS SGNLL |
| ADF p53 | FRHSVVVPYEPPEVGS DCTTIHYNMCMNSSCMGGMNRRPILTIITLEDSSGNLL |
| h p53 | 266 G RNSFEVRVCACPGRDRRTEENLRKKGEPHHELP PGSTKRALPNNTSSSPQP |
| ADF p53 | E RNSFEVRVCACPGRDRRTEENLRKKGEPHHELP PGSTKRALPNNTSSSPQP |
| h p53 | KKKPLDGEYFTLQIRGRERFEMFRELNEALEL KDAQAGKEPGGSR AHS SHLKS |
| ADF p53 | KKKPLDGEYFTLQIRGRERFEMFRELNEALEL KDAQAGKEPGGSR AHS SHLKS |
| h p53 | KKGQSTSRHKKLMFKTEGPDS DZ-394 |
| ADF p53 | KKGQSTSRHKKLMFKTEGPDS DZ-394 |

Figure 7

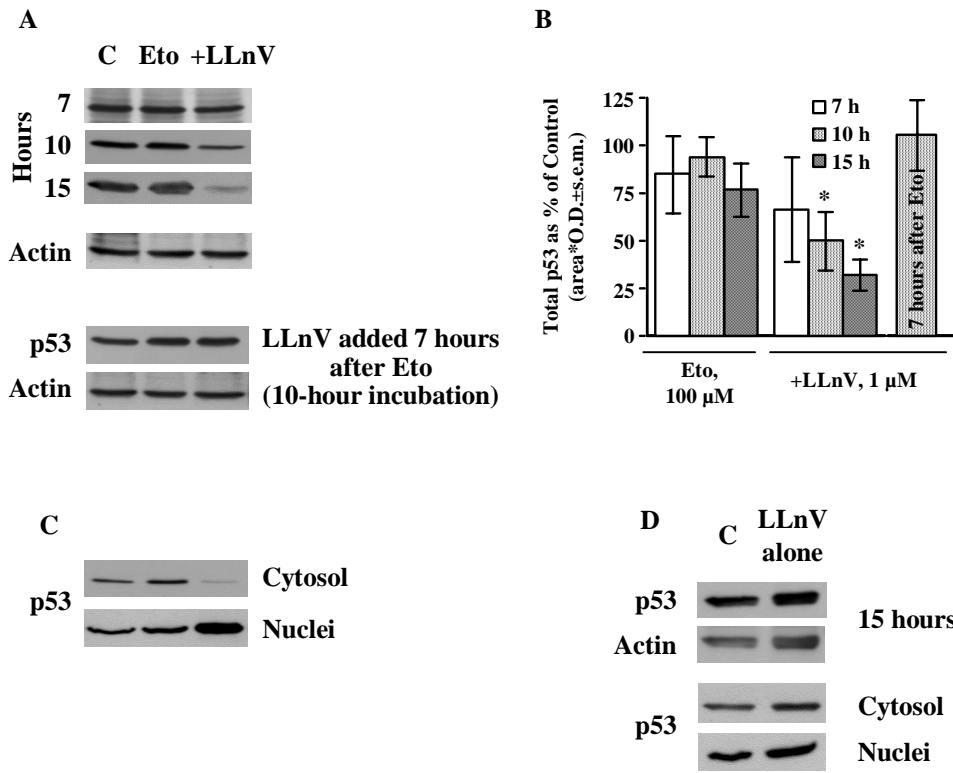


Figure 8

